Fourier transform infrared characterization of nanometre SnO$_2$

Hao Zhang†‖, Yulong Liu†, Ke Zhu†, Gueigu Siu‡, Yonghong Xiong§ and Caoshui Xiong§

† Laboratory of Optical Physics, Institute of Physics, Chinese Academy of Sciences, PO Box 603, Beijing 100080, People's Republic of China
‡ Department of Physics and Materials Science, City University of Hong Kong, Tat chee Avenue, Kowloon, Hong Kong, People's Republic of China
§ Structure Research Laboratory, University of Science and Technology of China, Chinese Academy of Sciences, Hefei, Anhui 230026, People's Republic of China

Abstract. Fourier transform infrared transmission and reflectance spectra of nanometer SnO$_2$ with particle sizes ranging from 4 to 80 nm have been recorded at room temperature. The results show that even in very small sizes (4–8 nm), the grains retain the main features of rutile structure. Two surface modes at 640 and 520 cm^{-1} without specific symmetries have been identified. The peak at 550 cm^{-1} manifests the lattice imperfections in bigger nanometre samples. The present results indicate that the FT-IR technique is more sensitive than Raman scattering in the characterization of the transformation from nano-grains to polycrystalline.

Stannic oxide (SnO$_2$) has excellent photoelectronic properties and sensitivities to gases which has attracted much research on its physics and chemistry [1–4]. Nanometre SnO$_2$ possesses some different characteristics from crystalline [5, 6] and has found applications in gas sensor technology [7]. An earlier work on Raman scattering in nano-SnO$_2$ related some micro-structural changes of grains and the change of space symmetry with the annealing temperature [8]. Fourier transform infrared spectroscopy (FT-IR) has been widely used in the morphology characterization of many oxides and ceramic materials, since IR spectra are very sensitive to local lattice distortions and bond strength [9–11]. It has been proposed that [10, 11], due to its somewhat larger probing depth, the IR spectra may be more sensitive than x-ray diffraction (XRD) and Raman spectroscopy in the characterization of phases and lattice distortions. In this paper, we report FT-IR spectra of nano-SnO$_2$ with particle sizes ranging from 4 to 80 nm. The subtle spectral features manifest the transformation from nanometre grains to heterogeneous morphologies.

The nano-SnO$_2$ grains with an average grain diameter smaller than 4 nm were obtained by the hydrothermal method [8, 12]. The powder was dried in a vacuum desiccator and then stored in a desiccator. Under a pressure of 200 MPa, the nano-SnO$_2$ powder was pressed to form circular discs with a diameter of about 10 mm and a thickness of about 1 mm. Isothermal annealing at 473, 673, 873, 1073 and 1273 K for 6 hours yielded samples with average grain sizes of 4, 8, 20, 40 and 80 nm, respectively, as determined by both TEM micrograph and the XRD Scherrer formula [8] (the samples including the as-formed one are denoted by n-1, n-2, . . . , n-6 respectively). Structural analysis shows that a large number of

‖ Present address: Physics Department, University of Miami, Coral Gables, FL 33124, USA. E-mail address: hzhang@phyvax.ir.miami.edu.

vacancies of oxygen, vacancy clusters and local lattice disorders are present in unannealed samples [8]. As the annealing temperature increases, the lattice defects begin to disappear. When the particle size reaches 80 nm, both the XRD and Raman spectra show that the materials have the main properties of polycrystals. The FT-IR measurements employed two spectrometers: a Bio-Rad FTS 6000 with a KBr beam-splitter and a TGS detector in the mid-IR range (4000–400 cm^{-1}) and a Bio-Rad FTS 60V in the far-IR range. Both a Mylar beam-splitter (500–50 cm^{-1}) and a metal wire mesh (700–50 cm^{-1}) were used in the far-IR range for comparison. The resolution was better than 4 cm^{-1}. In FT-IR transmission measurements, the samples were dispersed both in KBr and CsI for comparison. In FT-IR reflectance measurement, a mirror of gold thin film served as the reference; both the sample and the reference were recorded in a single beam, then their ratio was expressed as the infrared-reflectance spectra. All of the spectral measurements were carried out at room temperature.

Stannic oxide has rutile structure with space group $P4_2/mnm$ and point group D$_{4h}$. The spectral studies on single crystal [13, 14], polycrystals [15–17] and lattice dynamical calculations [14, 18] give the zone centre IR active modes as: 3E$_u$ at 244 cm^{-1} (TO), 276 cm^{-1} (LO), 293 cm^{-1} (TO), 366 cm^{-1} (LO), 618 cm^{-1} (TO), 770 cm^{-1} (LO); A$_{2u}$ at 477 cm^{-1} (TO), 705 cm^{-1} (LO).

Figure 1 shows the FT-IR transmission spectra of nano-SnO$_2$ dispersed in CsI. Figure 2 is that dispersed in KBr (only the mid-IR range is reliable for KBr pellets). The striking feature is that even in very small grains (4–8 nm) the samples are shown to have rutile structure especially manifested in the far-IR range, while their Raman spectra hardly show rutile characters [8]. This shows that the IR spectra are more sensitive to short range order than Raman spectra [17]. Two bands around 254 and 300 cm^{-1} are obviously two E$_u$ type modes. Since the E$_u$ modes are related to relative displacements of Sn and O ions vertical to the crystal c axis [16], the above results show that the x–y plane movements and bond strength of Sn and O ions in nano-SnO$_2$ have little differences from those of crystals.

In the mid-IR region, the spectra undergo a significant change at the n-3 sample. In n-1 and n-2 samples, two dominant absorbance peaks around 660 and 516–540 cm^{-1} are attributed to surface phonons, since the increase of the medium dielectric constant (from KBr ($\varepsilon_m = 2.36$) to CsI ($\varepsilon_m = 2.6$)) leads to a downshift of their positions [19]: the 663 cm^{-1} peak shifts to 659 cm^{-1} and the 538 cm^{-1} peak shifts to 517 cm^{-1}, as shown in figure 3(a); while the bulk mode appearing in higher temperature treated samples (above 873 K, E$_u$(TO) $\sim$ 619 cm^{-1}) is unchanged, as shown in figure 3(b). An estimation of the surface mode frequencies is given by [19]:

$$\frac{\omega^s_{A_{2u}}}{\omega_{A_{2u}}(\text{TO})} = \left(\frac{\varepsilon_{0\parallel} + \varepsilon_m}{\varepsilon_{\infty\parallel} + \varepsilon_m} \right)^{1/2} \tag{1}$$

$$\prod_{j=1}^{3} \frac{\omega^{sj}_{E_u}}{\omega^j_{E_u}(\text{TO})} = \left(\frac{\varepsilon_{0\perp} + \varepsilon_m}{\varepsilon_{\infty\perp} + \varepsilon_m} \right)^{1/2} \tag{2}$$

where the ω^s are frequencies of surface phonons; $\parallel$ means the direction parallel to the c axis and $\perp$ the perpendicular ones. Using the optical parameters given by Luxon and Summitt [15], the right-hand sides of equations (1) and (2) give the value of 1.353 and 1.556 for KBr, 1.342 and 1.538 for CsI, respectively. For A$_{2u}$(TO) = 477 cm^{-1}, equation (1) predicts its surface phonons locate at 645 cm^{-1} (KBr) and 640 cm^{-1} (CsI). However, if the peak around 660 cm^{-1} is assigned to be A$_{2u}$ type, the other around 520 cm^{-1} can be assigned to none of the remaining E$_u$ type modes, since one of the characteristic properties of surface phonons is that they appear between the bulk TO and LO modes. Then it is
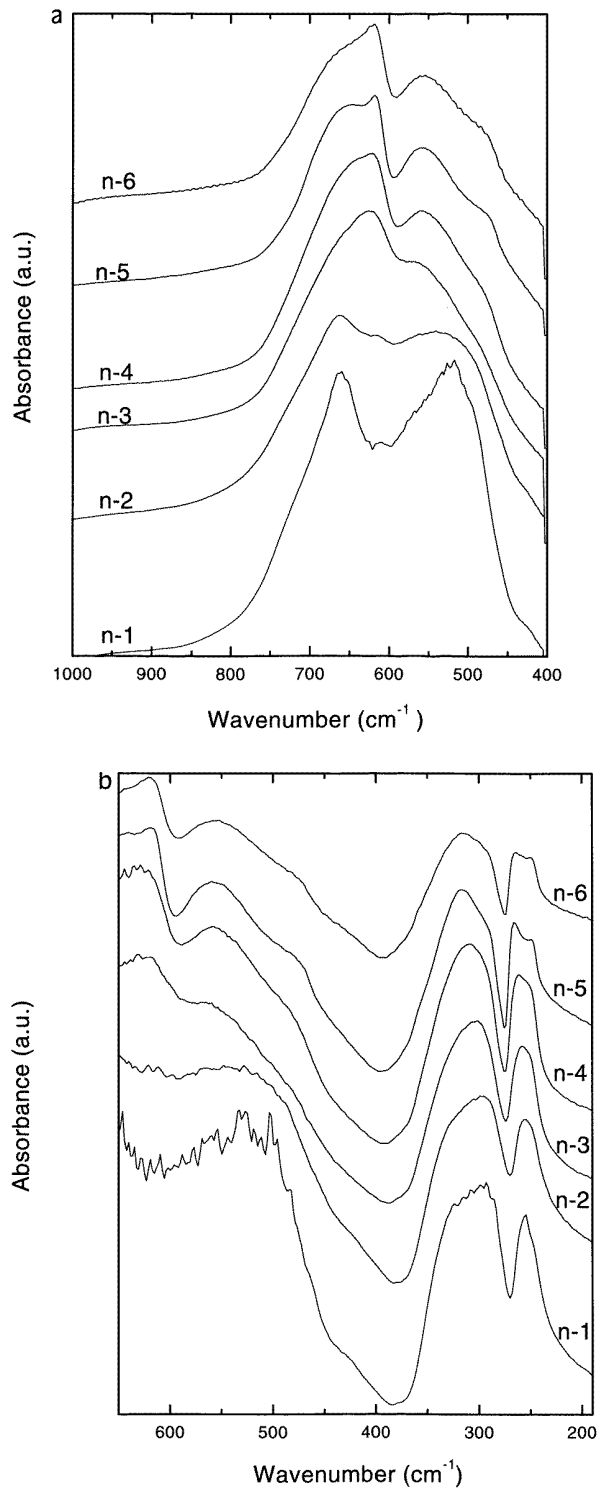
Figure 1. FT-IR transmission spectra of nanometre-SnO$_2$ samples dispersed in CsI. (a) Mid-IR region; (b) far-IR region; see text for the corresponding particle size.
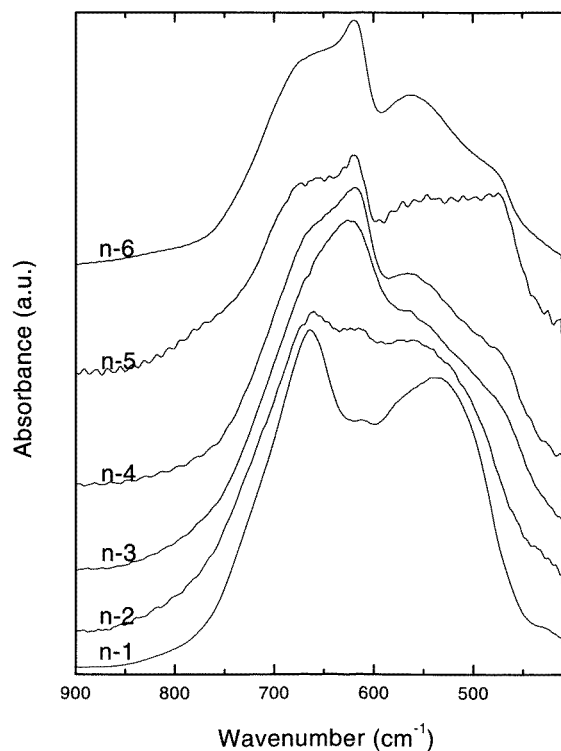
Figure 2. FT-IR transmission spectra of nanometre-SnO$_2$ samples dispersed in KBr.

supposed that, due to the lattice distortions and vacancy sites in nano-SnO$_2$, the E$_u$ mode (TO $= 618$ cm^{-1}, LO $= 770$ cm^{-1}) relating the vertical relative displacements of Sn and O ions has 'mixed' with the A$_{2u}$ mode which relates their parallel relative displacements [16] because of their overlapping vibration eigenfrequencies. Thus the 660 and 520 cm^{-1} surface bands do not have purely specific symmetries. At annealing temperature 673 K, the spectra of n-3 takes an appearance between n-2 and n-4, having a broad peak around 630 cm^{-1} with a shoulder around 550 cm^{-1}, showing the sample nature is changing from nanograin to bulk-like. According to the theory of average dielectric constant (TADC) [17], the 630 cm^{-1} peak is the indication of the presence of oblate spheroids in the sample, and the 550 cm^{-1} peak represents the mixture of particles of several morphologies; at 673 K annealing temperature, the nanometre assemblage begins to aggregate to form bigger size clusters; the oblate spheroids must appear; at higher annealing temperatures, some large plate-like morphologies must further appear; thus the mixture accounts for the 550 cm^{-1} band, as will be seen again in reflectance spectra below. At 873 K annealing temperature, the E$_u$(TO) at 619 cm^{-1} and the A$_{2u}$(TO) at 480 cm^{-1} appear and 'grow up', showing more bulk characters. The n-6 sample was characterized by Raman spectra as well crystallized [8]; however, the existence of the 550 cm^{-1} band in its infrared spectra shows the existence of structural defects in the nearly polycrystalline lattice. Again, FT-IR spectra show greater sensitivity.

Figure 4 shows the reflectance spectra of nano-SnO$_2$. The spectrum of a polycrystalline sample (average particle size $\sim$0.2 μm) was also recorded for comparison. It is notable that both of the band positions and shapes of the IR reflectance spectra correlate to their
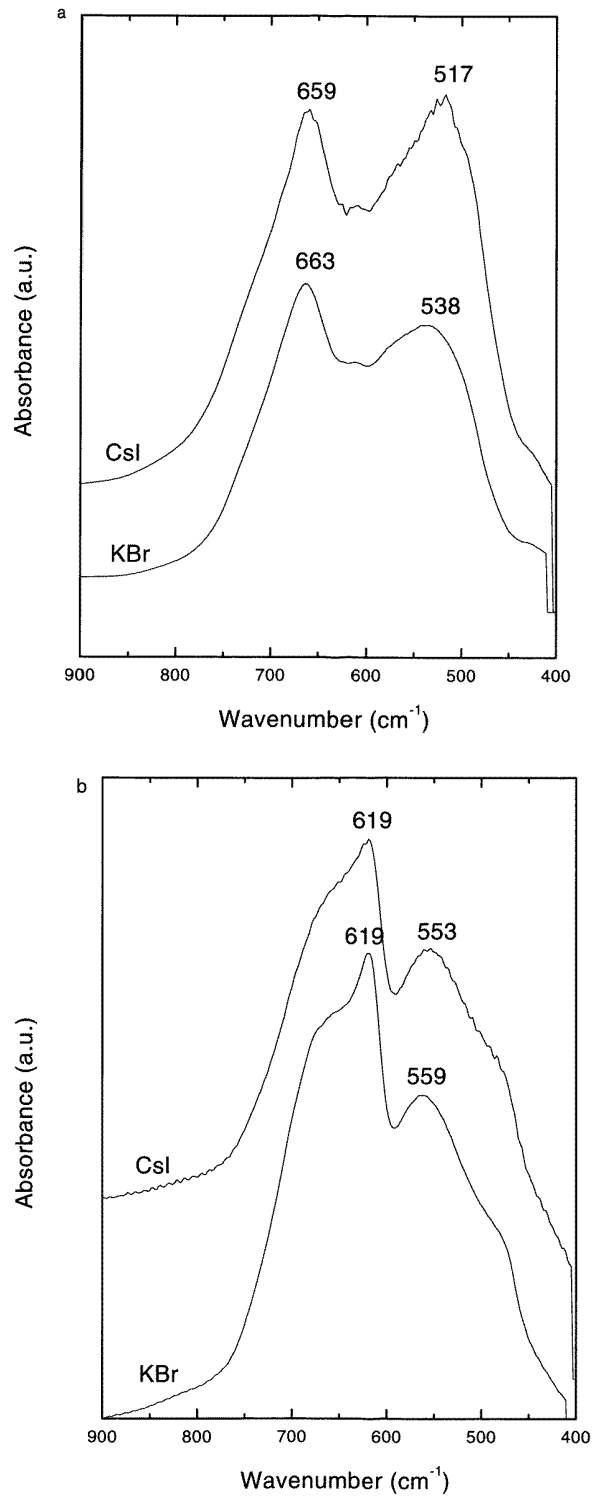
Figure 3. Comparison of FT-IR transmission spectra of the same dispersed in CsI and KBr:
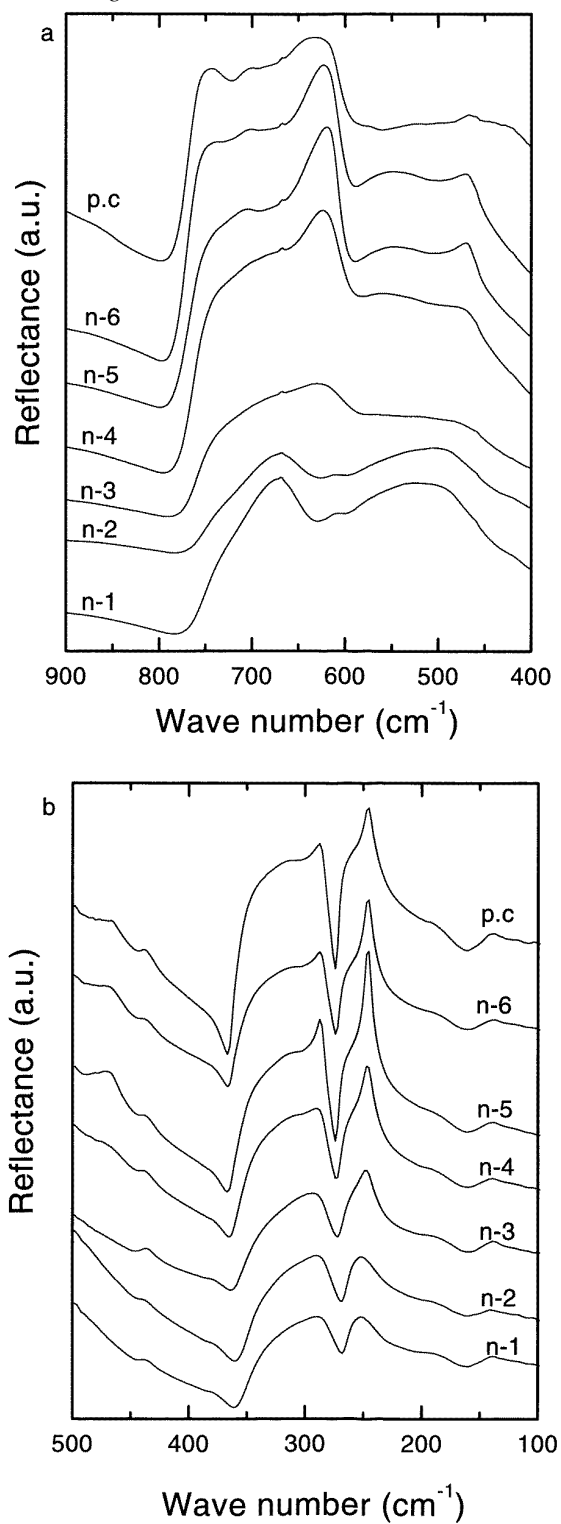(a) n-1 sample (4 nm); (b) n-6 sample (80 nm).

Figure 4. FT-IR reflectance spectra of nanometre-SnO_2 samples. (a) Mid-IR region; (b) far-IR region; 'p.c.' means polycrystalline.

corresponding transmission spectra; this is true for many inorganic compounds [10]. The reflectance bands in the mid-IR range (figure 4(a)) vary greatly from the n-2 to the n-3 sample while that in the far-IR region (figure 4(b)) undergo little change; the reason is discussed in the above transmission spectra. It is interesting to note that the reflectance maxima sharpen as the particle size increase; at the same time the 'dips' around 270, 360 and 800 cm^{-1} shift to higher wavenumber. It was pointed out that most infrared powder spectra of rutile (TiO$_2$) actually correspond to that of a heterogeneous material [20]. For example, the IR absorbance bands around 720, 600, 535 cm^{-1} of rutile powders correspond to the contributions of plate-like morphologies, spheres and oblate spheroid particles, respectively [20]. From the discussions on transmission spectra, it is clear that similar situations apply for SnO$_2$ powders. Obviously, as the annealing temperature increases, the isolated nanometre spheres would grow bigger, forming some oblate spheroids ($\sim$630 cm^{-1} in n-3); then, as the particles merge into bigger sizes, the plate-like morphologies must appear and the sample accommodates heterogeneous morphologies ($\sim$550 cm^{-1}), further approaching polycrystals (whose spectrum, however, does not have the 550 cm^{-1} band, showing its better lattice perfection). When the sample is well crystallized and ordered, the long range macroscopic electric field works more significantly during lattice vibrations and the longitudinal E$_u$(LO) polar modes appear (e.g. the 700–750 cm^{-1} bands) [16], broadening the reflectance bands in the higher frequency side, thus shifting the dips.

In conclusion, the FT-IR transmission and reflectance spectra manifest subtle structural changes from nanometre spheroids to heterogeneous samples including oblate spheroids and plate-like morphologies. The present results indicate the FT-IR technique is more sensitive in the characterization of the transformation from nanometre grains to polycrystalline compared with Raman spectra. Since there is good correspondence between the reflectance spectra and the transmission spectra both in band positions and shapes, while the reflectance measurement can be applied to as-formed samples, the present study shows FT-IR reflectance measurement is a powerful tool in the characterization of inorganic nanometre assemblage.

References

[1] Miyasaka T 1979 *Nature* **277** 638
[2] Ogawa H 1981 *J. Electrochem. Soc.* **128** 2020
[3] Nitta M 1980 *J. Electrochem. Mater.* **9** 127
[4] Smay G L and Wasylyk J S 1981 *Glass Technol.* **22** 2516
[5] Ishida T 1994 *J. Electrochem. Soc.* **141** 1357
[6] Bedja I, Hotchandani S, Carpentier R, Fessenden R and Kamat P 1994 *J. Appl. Phys.* **75** 5444
[7] Gopel W and Reinhardt G 1996 *Sensors Update* vol 1, ed H Baltes, W Gopel and J Hesse (Weinheim: VCH)
[8] Yu K N, Xiong Y H, Liu Y L and Xiong C S 1997 *Phys. Rev.* B **55** 2666
[9] Hirata T 1994 *Phys. Rev.* B **50** 2874
[10] Phillippi C M and Mazdiyasni K S 1971 *J. Am. Ceram. Soc.* **54** 254
[11] Hirata T, Asari E and Kitajima M 1994 *J. Solid State Chem.* **110** 201
[12] Xiong Y H, Yu K N and Xiong C S 1994 *Phys. Rev.* B **49** 5607
Xiong Y H, Yu K N and Xiong C S 1994 *Phys. Rev.* B **50** 11 287
[13] Katiyar R S, Dawson P, Hargreave M M and Wilkinson G R 1971 *J. Phys. C: Solid State Phys.* **4** 2421
[14] Sato T and Asari T 1995 *J. Phys. Soc. Japan* **64** 1193
[15] Luxon J T and Summitt R 1969 *J. Chem. Phys.* **50** 1366
[16] Hirata T, Ishioka K, Kitajima M and Doi H 1996 *Phys. Rev.* B **53** 8442
[17] Ocana M, Serna C J, Ramos J V G and Matijevic E 1993 *Solid State Ion.* **63–65** 170
[18] Gervais F and Kress W 1985 *Phys. Rev.* B **31** 4809
[19] Ruppin R 1982 *Electromagnetic Surface Modes* ed A D Boardman (New York: Wiley) ch 2
[20] Ocana M, Fornes V, Ramos J V G and Serna C J 1988 *J. Solid State Chem.* **75** 364